

# Supplementary Information

## S1 Description of speciation criterion

We introduce a simple speciation metric,  $S$ , that measures the degree to which the population has bifurcated at the genetic loci underlying the ecological trait. We only calculate this metric across the 10 genetic loci in order to control for locus number when making comparisons between “additive” and “redundant” maps. An individual’s ecological phenotypic trait value calculated at a subset of 10 genetic loci is

$$x_{\text{gen}} = \sum_{i=1}^{10} x_{i;\text{gen}} \quad (\text{S1})$$

Across the population, we denote the median value of  $x_{\text{gen}}$  by  $\tilde{x}_{\text{gen}}$ . In words, our speciation metric is calculated as the fraction of the population whose value of  $x_{\text{gen}}$  is equal to  $\tilde{x}_{\text{gen}}$ . Specifically, the speciation criterion,  $S$  is defined as

$$S = \frac{\sum_{j=1}^{2 * K} i_j}{2 * K} \quad (\text{S2})$$

where the sum is over all  $2 * K$  individuals in the population, and  $i_j$  is an indicator variable for individual  $j$  whose ecological phenotypic trait value is  $x_{\text{gen},j}$ , for which

$$i_j = \begin{cases} 1, & \text{if } x_{\text{gen},j} = \tilde{x}_{\text{gen}} \\ 0, & \text{otherwise.} \end{cases} \quad (\text{S3})$$

When this speciation metric is high, it means that there is plenty of interbreeding between individuals with high and low ecological trait values (i.e., the population is close to panmixia); however, when it is low, the subsets of the population with high and low

615 ecological trait values are not frequently interbreeding (i.e., that there is assortative mat-  
616 ing). We define speciation to occur when this metric drops below a threshold value of  
617  $S = 0.1$ .

## 618 **S2 Description of Assortative Mating Index**

619 We introduce an index, AMI, that measures the degree to which individuals are mating  
620 assortatively with respect to ecological genotypes. When this index is small, assortative  
621 mating is uncommon and when it is large, assortative mating is common.

622 We begin with the value  $\tilde{x}_{\text{gen}}$  calculated in Section S1. For each mating pair, we then  
623 calculate the ecological trait value at the same subset of genetic loci for the father,  $x_{\text{gen}}^{\text{father}}$ ,  
624 and for the mother,  $x_{\text{gen}}^{\text{mother}}$ . AMI then quantifies the fraction of matings in which mothers'  
625 and fathers' ecological values are both on the same side of the median,  $\tilde{x}_{\text{gen}}$ . Specifically:

$$\text{AMI} = \frac{\sum_{p=1}^M i_p}{M} \quad (\text{S4})$$

626 where the sum is over all  $M$  mating pairs, and  $i_p$  is an indicator variable for mating pair  
627  $p$  for which

$$i_p = \begin{cases} 1, & \text{if } (x_{\text{gen},p}^{\text{father}} - \tilde{x}_{\text{gen}}) * (x_{\text{gen},p}^{\text{mother}} - \tilde{x}_{\text{gen}}) > 0 \\ 0, & \text{otherwise.} \end{cases} \quad (\text{S5})$$

628

### 629 **S3 Alternative systems for epigenotype & genotype to phe-** 630 **notype mapping**

631 We separately consider two different maps from genetic and epigenetic states to pheno-  
632 type. The first, which we refer to as the “additive” map is described in the main text. The  
633 other, which we term the “redundant” map, is based on the notion that similar pheno-  
634 types can be attained through alternative means (i.e., genetics vs phenotypic plasticity).  
635 Each genetic locus is assumed to be redundant in its phenotypic effect with exactly one  
636 epigenetic locus. In the extreme, it is therefore possible to reach any phenotype through  
637 only genetic or only epigenetic change. For our purposes, the important difference be-  
638 tween these maps is that in the redundant map (but not the additive map), there is inter-  
639 ference between the genetic and epigenetic systems because every genetic allele’s effect  
640 can be accomplished by an epigenetic marker.

641 Under the redundant map, we calculate the ecological phenotype of an individual,  $x$ ,

642 as

$$x = \frac{\sum_i^{n_{\text{ecol}}} \max(x_i^{\text{genetic}}, x_i^{\text{epigenetic}})}{n_{\text{ecol}}}, \quad (\text{S6})$$

643 where both  $x_i^{\text{genetic}}$  (which represents the contribution of genetic allele  $i$ ) and  $x_i^{\text{epigenetic}}$   
644 (which represents the contribution of epiallele  $i$ ), take values of 0 or 1. The number of  
645 genetic loci and epigenetic markers are necessarily equal (with  $n_{\text{ecol}} = 20$ ) and we set  
646 both equal to the total number of loci used in our additive map.

### 647 **S4 Soft selection regime**

648 We separately consider “hard” and “soft” selection regimes. Under hard selection an in-  
649 dividual’s survival probability is given by its fitness  $w_{x;k;j}$  whereas, under soft selection,  
650 we sample individuals, with replacement to create a new pre-mating population, where

651 each individual's probability of being sampled is proportional to its fitness  $w_{x;k;j}$ . The  
652 latter case is a Wright-Fisher process with selection. Despite it not being ecologically real-  
653 istic, we implement the soft selection regime in order to remove the effects of bottlenecks  
654 that occur in the more realistic hard selection regime; by comparing the two regimes we  
655 can infer the effect of bottlenecking.

656 **S5 Supplementary Tables & Figures**

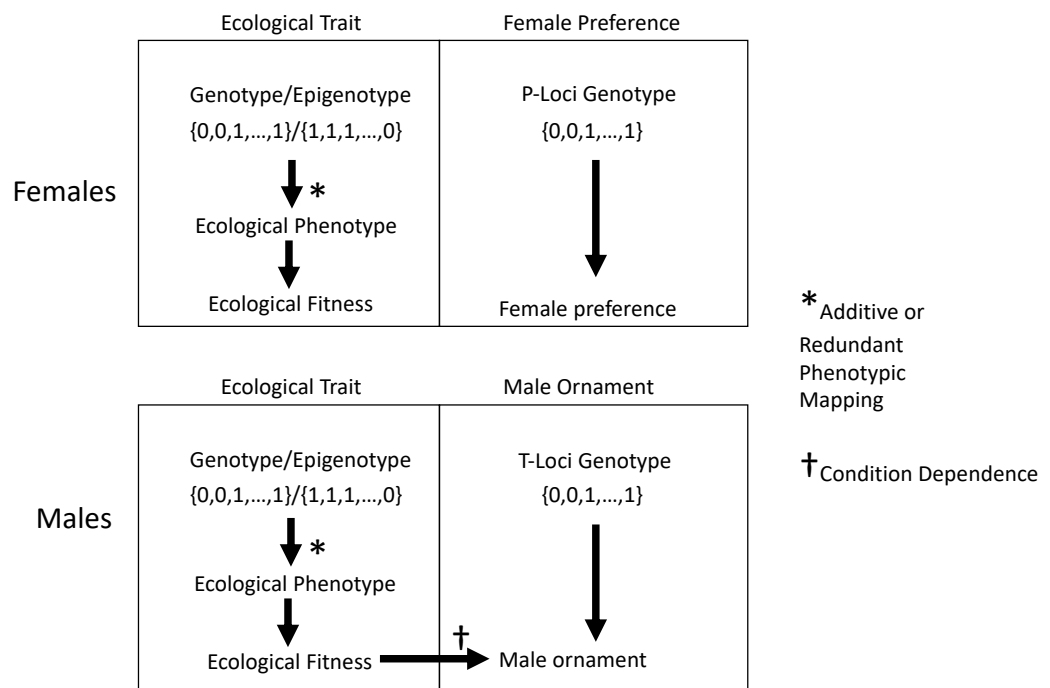


Figure S1: For each individual of the population, genotype and epigenotype is mapped onto phenotype.

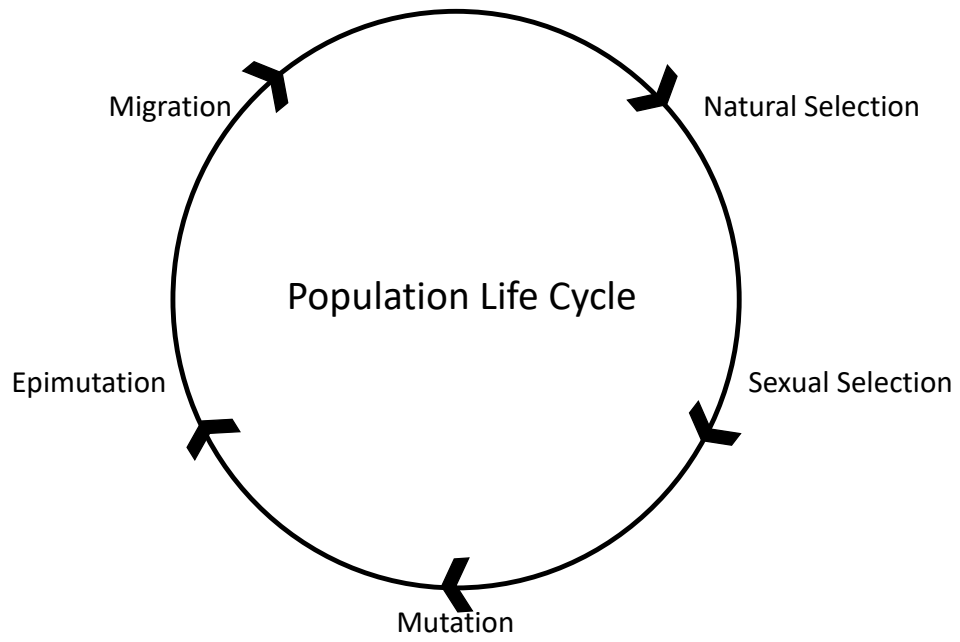


Figure S2: The life cycle of the population. For information about each stage, see the Materials and Methods section.



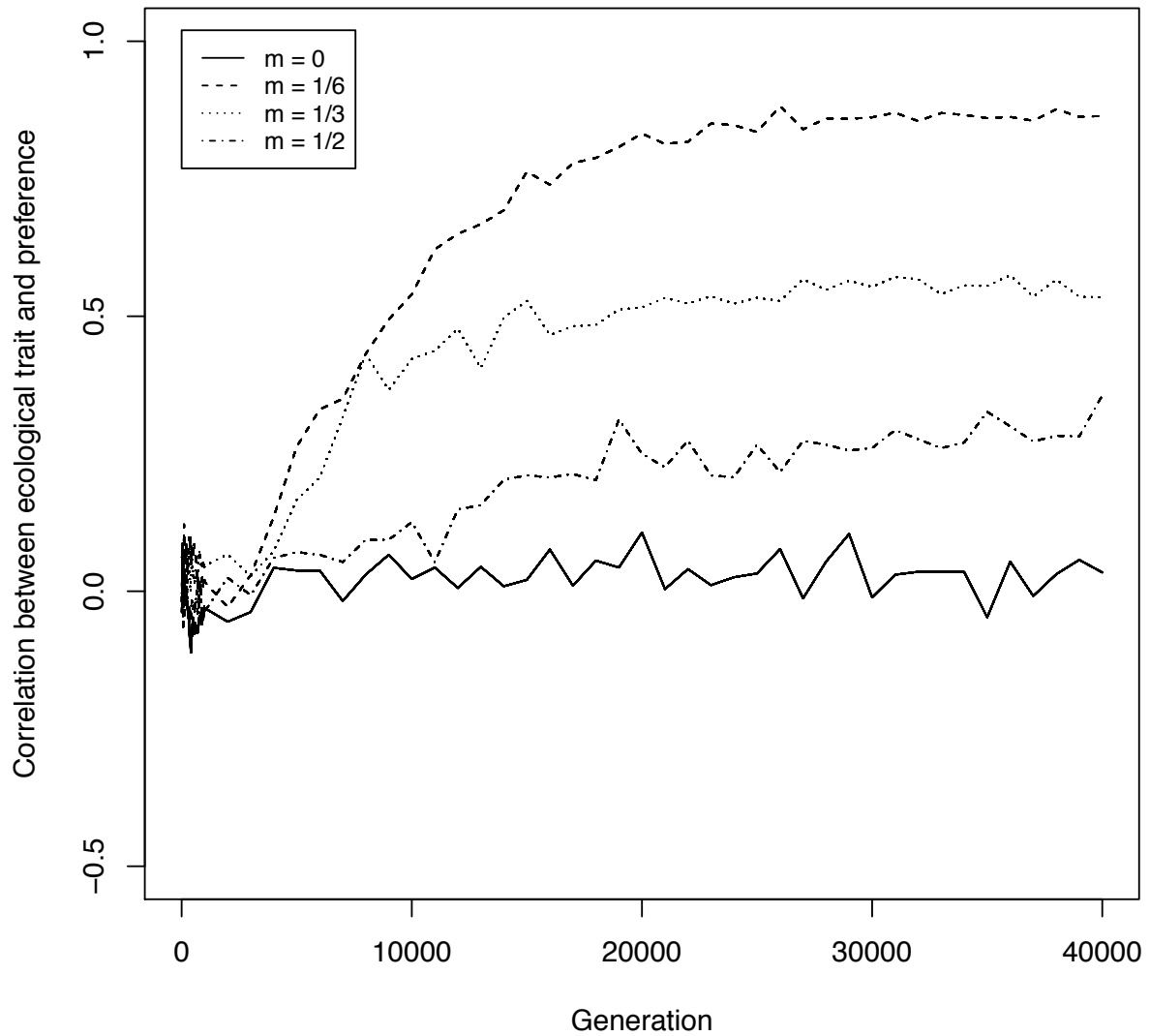


Figure S3: The correlation between the strength of the female preference and the locally adapted genotype over time in patch 1. For each parameter set  $p$ , we calculated across replicates,  $r$ , the Pearson correlation coefficient,  $\rho_{g,a} = \text{cor}_r(g, a)$  between the proportion,  $g$ , of locally adapted 1 alleles across all genetic loci of all individuals and the average female preference,  $a$ , across all individuals. Shown are the correlations across 35 replicates averaged over values of  $\tau$  and separated by migration rate,  $m$ .

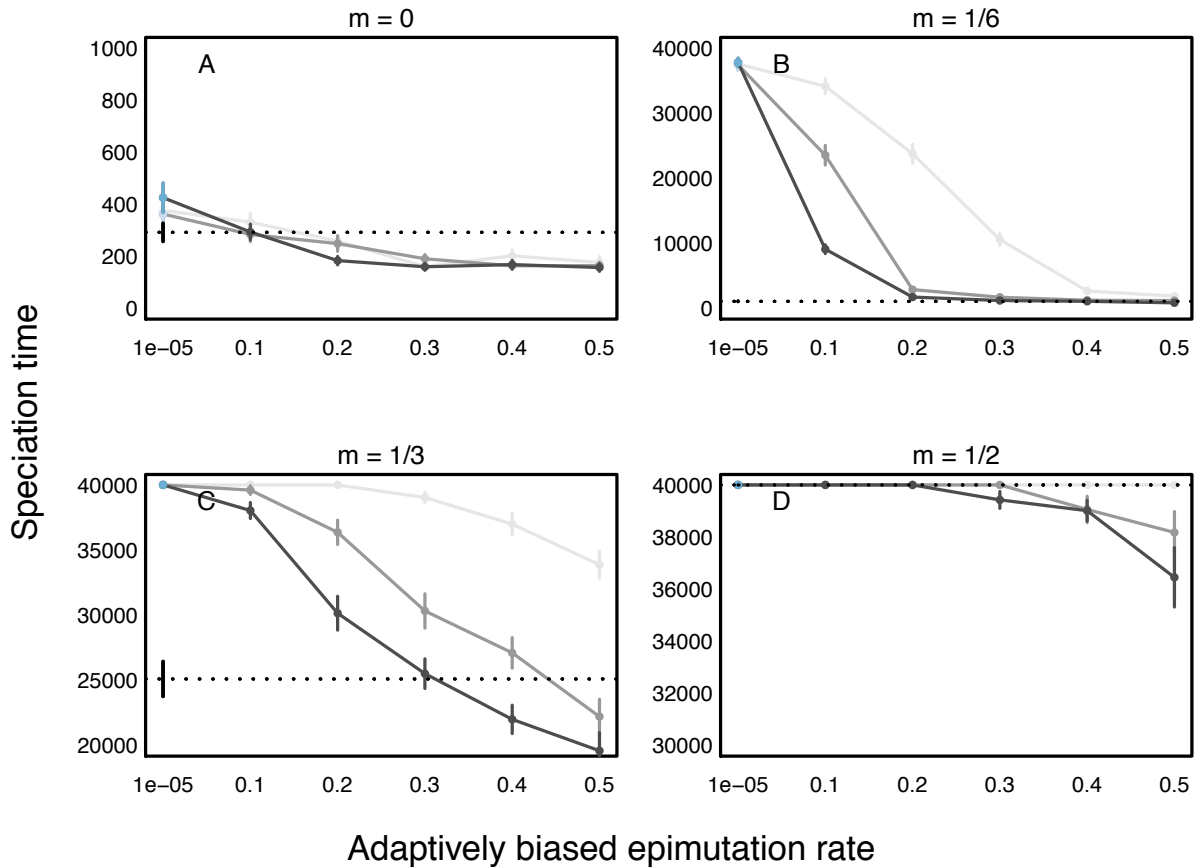


Figure S4: Time to speciation is generally shorter for higher rates of adaptively-biased epimutation ( $\mu_{\text{epi};A}$ ) when selection is weak. All specifications are as in Fig. 2 except that here  $\sigma = 0.4$  (compared to  $\sigma = 0.35$ , there). Points show mean speciation time when epigenetic induction is adaptively biased (black) or unbiased (blue; adaptively biased epimutation rate and maladaptive epimutation rate are both equal to  $10^{-5}$  for left-most points); error bars denote standard error. Each point represents the average over 35 replicate model runs. The dotted line shows the time to speciation for a model with 20 genetic loci and no epigenetic loci, and its standard error is displayed as a bar on the left side. Parameters values are listed in Table 1, except  $\sigma = 0.4$ , with  $\tau = 1$  (light grey),  $\tau = 2$  (dark grey) and  $\tau = 3$  (black). Note the differing scales for the  $y$ -axes among panels.

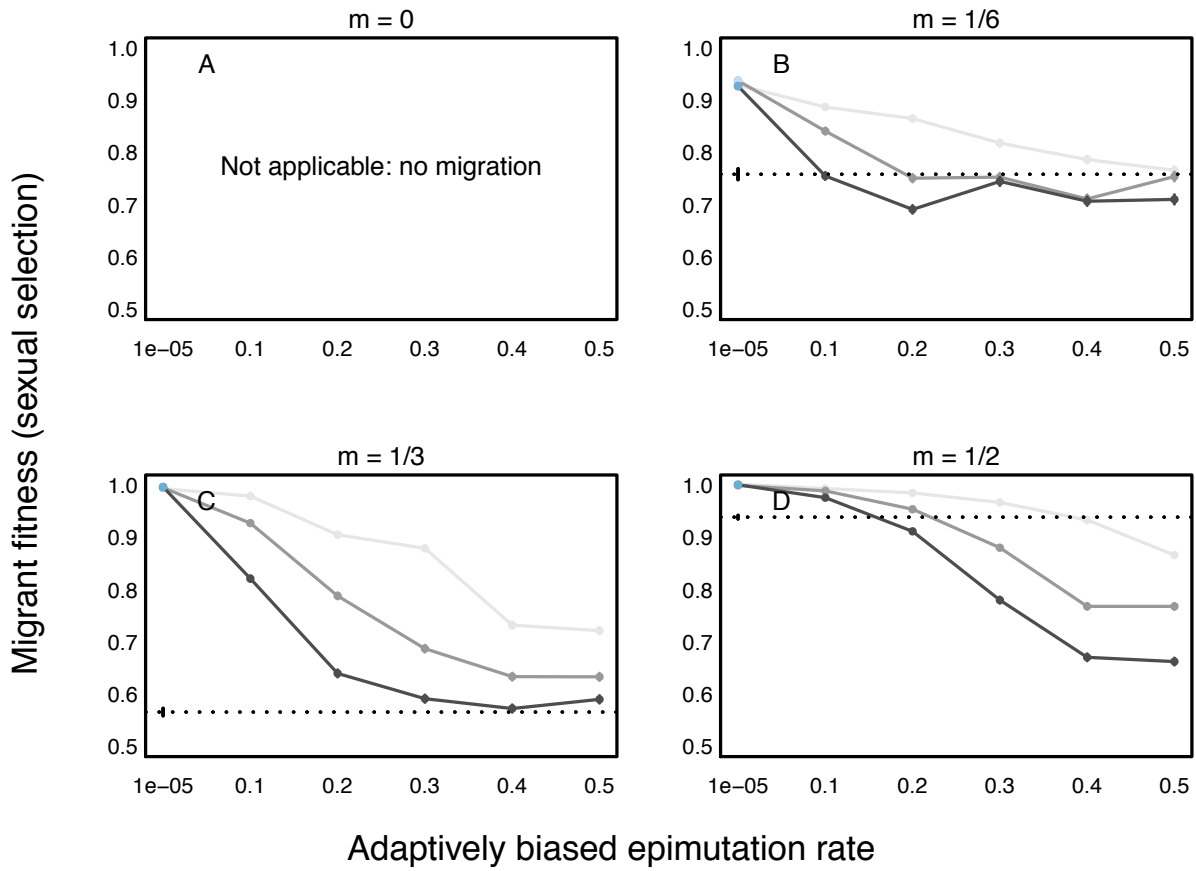


Figure S5: Mean migrant fitness due to sexual selection on males (averaged through time at evenly spaced time points) varies with the rate of adaptively-biased epimutation ( $\mu_{\text{epi};A}$ ) under our core model. Here, migrant fitness due to sexual selection is simply calculated from simulations as the ratio  $\frac{m_a}{m_b}$  where  $m_b$  is the frequency of migrants before the mate choice step and  $m_a$  is the fraction of migrants successfully chosen as fathers during mate choice. Points show mean fitness when epigenetic induction is adaptively biased (black) or unbiased (blue; adaptively biased epimutation rate and maladaptive epimutation rate are both equal to  $10^{-5}$  for left-most points); error bars denote standard error. Each point represents the average over 35 replicate model runs. The dotted line shows fitness for a model with 20 genetic loci and no epigenetic loci, and its standard error is displayed as a bar on the left side. Parameters values are listed in Table 1 with  $\tau = 1$  (light grey),  $\tau = 2$  (dark grey) and  $\tau = 3$  (black).

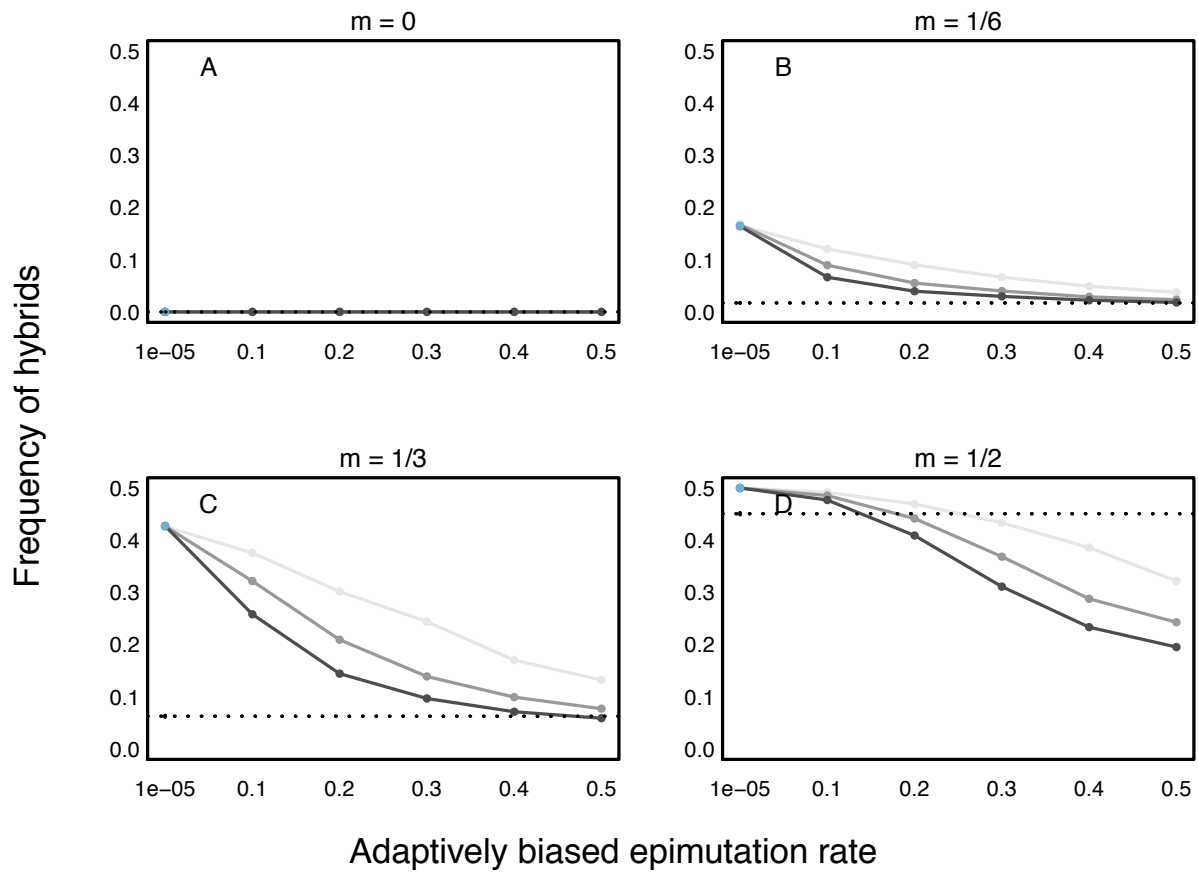


Figure S6: Mean hybrid frequency (averaged through time at evenly spaced time points) is generally lower for higher rates of adaptively-biased epimutation ( $\mu_{\text{epi};A}$ ) under our core model. Points show mean hybrid frequency when epigenetic induction is adaptively biased (black) or unbiased (blue; adaptively biased epimutation rate and maladaptive epimutation rate are both equal to  $10^{-5}$  for left-most points); error bars denote standard error. Each point represents the average over 35 replicate model runs. The dotted line shows hybrid frequency for a model with 20 genetic loci and no epigenetic loci, and its standard error is displayed as a bar on the left side. Parameters values are listed in Table 1 with  $\tau = 1$  (light grey),  $\tau = 2$  (dark grey) and  $\tau = 3$  (black).

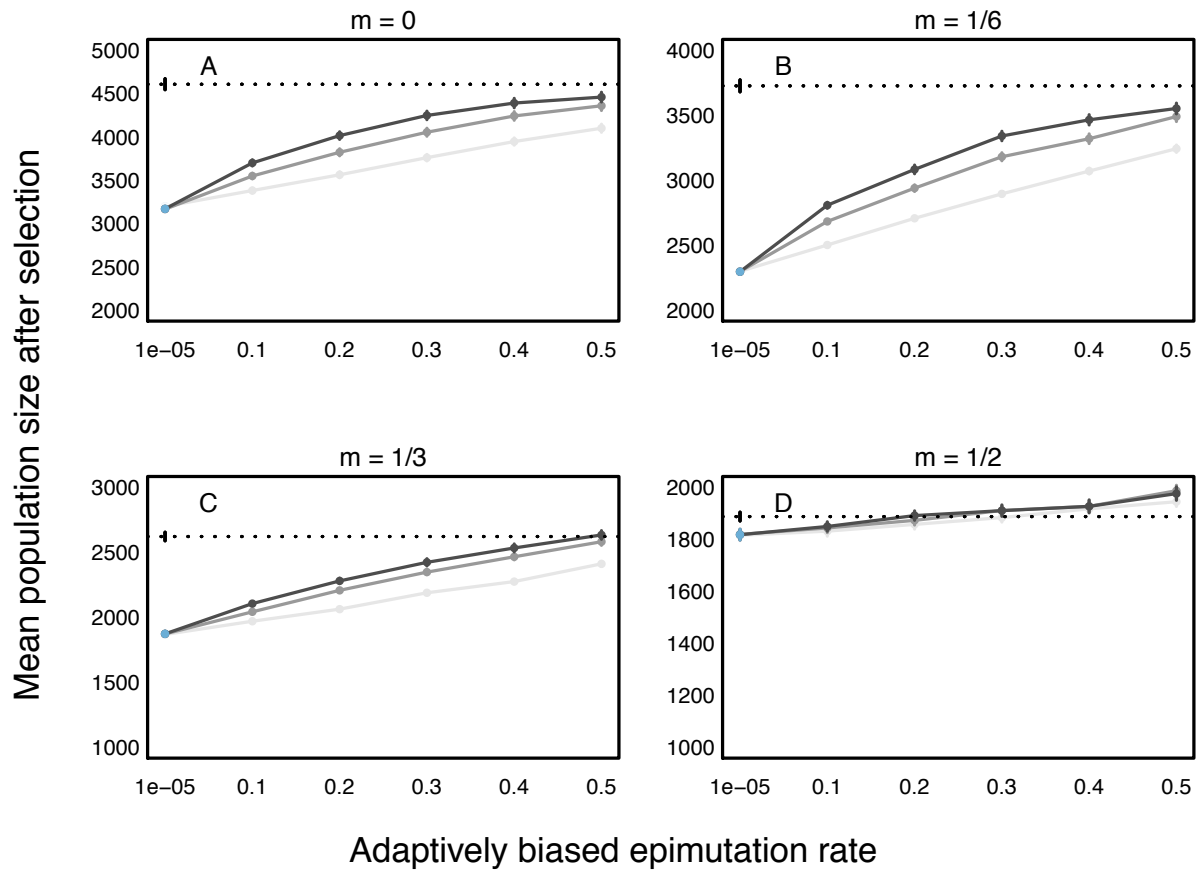


Figure S7: Mean population size after selection (averaged through time at evenly spaced time points) varies with adaptively-biased epimutation rate ( $\mu_{epi;A}$ ), demonstrating the bottlenecking that recurrently occurs under hard selection. Points show mean population size when epigenetic induction is adaptively biased (black) or unbiased (blue; adaptively biased epimutation rate and maladaptive epimutation rate are both equal to  $10^{-5}$  for left-most points); error bars denote standard error. Each point represents the average over 35 replicate model runs. The dotted line shows mean population size for a model with 20 genetic loci and no epigenetic loci, and its standard error is displayed as a bar on the left side. Parameters values are listed in Table 1 with  $\tau = 1$  (light grey),  $\tau = 2$  (dark grey) and  $\tau = 3$  (black). Note the differing scales for the  $y$ -axes among panels.

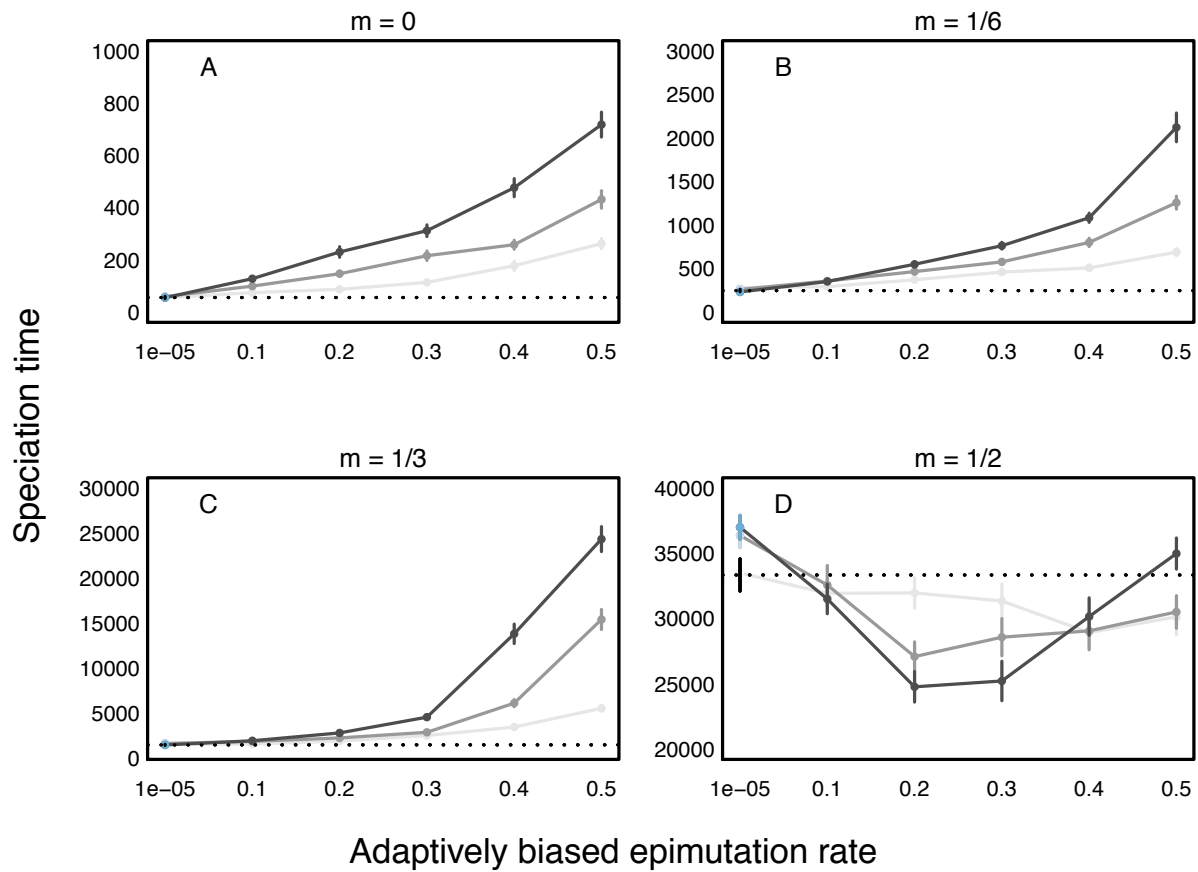


Figure S8: Time to speciation with soft selection under a redundant genotype/epigenotype to phenotype map. Points show mean speciation time when epigenetic induction is adaptively biased (black) or unbiased (blue; adaptively biased epimutation rate and maladaptive epimutation rate are both equal to  $10^{-5}$  for left-most points); error bars denote standard error. Each point represents the average over 35 replicate model runs. The dotted line shows the time to speciation for a model with 20 genetic loci and no epigenetic loci, and its standard error is displayed as a bar on the left side. Other parameters values were as listed in Table 1 with  $\tau = 1$  (light grey),  $\tau = 2$  (dark grey) and  $\tau = 3$  (black). Note the differing scales for the  $y$ -axes among panels.

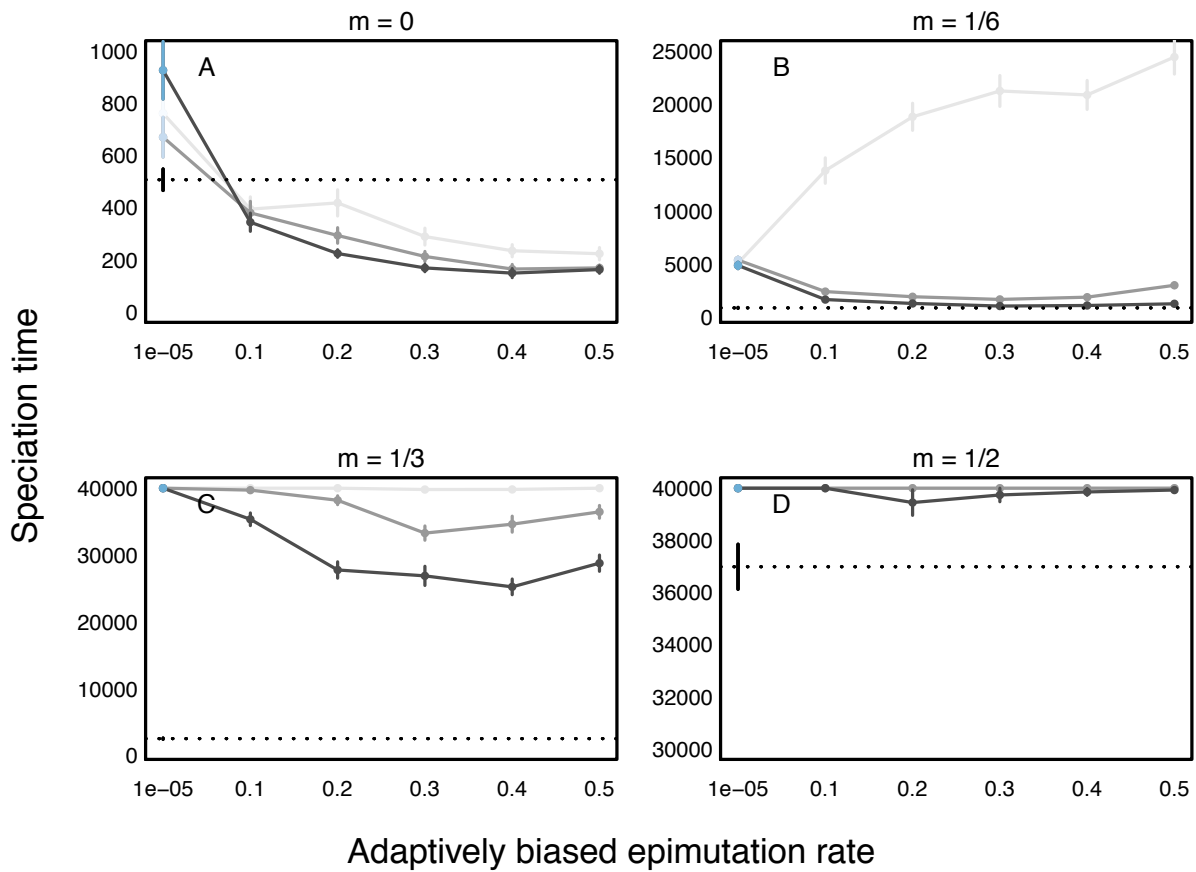


Figure S9: Time to speciation under our core model when genetic and epigenetic mutation happen *after* migration. Points show mean speciation time when epigenetic induction is adaptively biased (black) or unbiased (blue; adaptively biased epimutation rate and maladaptive epimutation rate are both equal to  $10^{-5}$  for left-most points); error bars denote standard error. Each point represents the average over 35 replicate model runs. The dotted line shows the time to speciation for a model with 20 genetic loci and no epigenetic loci, and its standard error is displayed as a bar on the left side. Other parameter values are as listed in Table 1 with  $\tau = 1$  (light grey),  $\tau = 2$  (dark grey) and  $\tau = 3$  (black). Note the differing scales for the  $y$ -axes among panels.

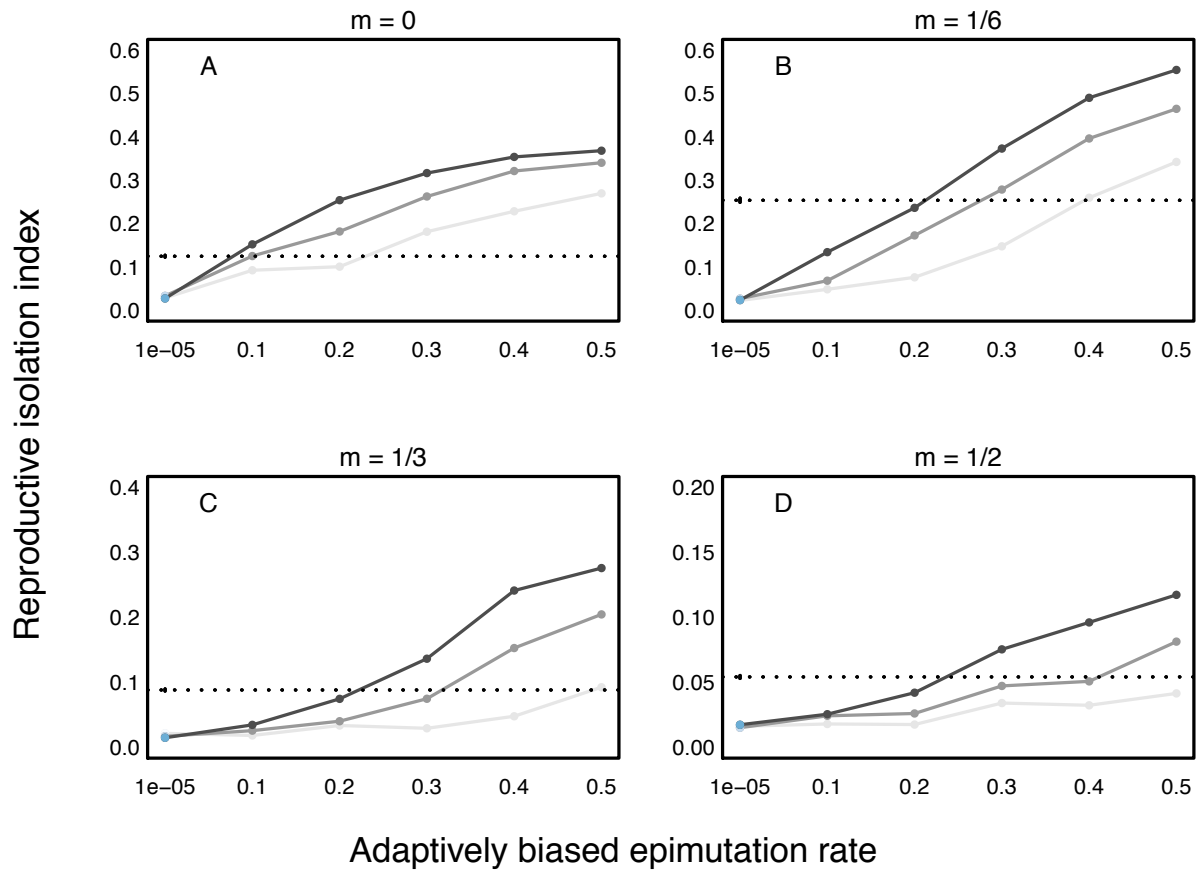


Figure S10: The assortative mating index (averaged through time over the first 1000 time steps at evenly spaced time points) defined in Section S2 under our core model. Points show mean index when epigenetic induction is adaptively biased (black) or unbiased (blue; adaptively biased epimutation rate and maladaptive epimutation rate are both equal to  $10^{-5}$  for left-most points); error bars denote standard error. Each point represents the average over 35 replicate model runs. The dotted line shows the index for a model with 20 genetic loci and no epigenetic loci, and its standard error is displayed as a bar on the left side. Other parameters values are as listed in Table 1 with  $\tau = 1$  (light grey),  $\tau = 2$  (dark grey) and  $\tau = 3$  (black). Note the differing scales for the  $y$ -axes among panels.



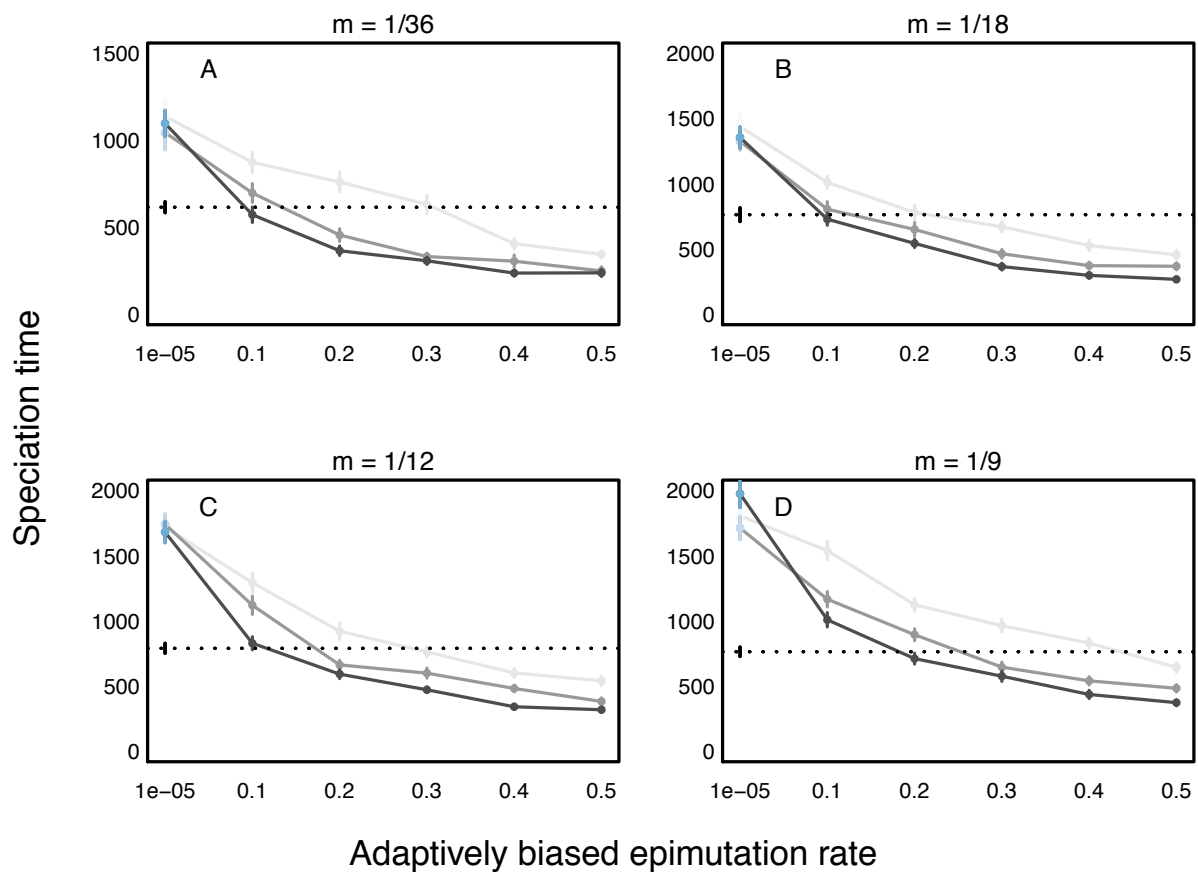


Figure S11: Analog of Fig. 2, but with lower migration rates. Parameters values are listed in Table 1 with  $\tau = 1$  (light grey),  $\tau = 2$  (dark grey) and  $\tau = 3$  (black). The dotted line shows the time to speciation for a model with 20 genetic loci and no epigenetic loci. Note the differing scales for the  $y$ -axes among panels.

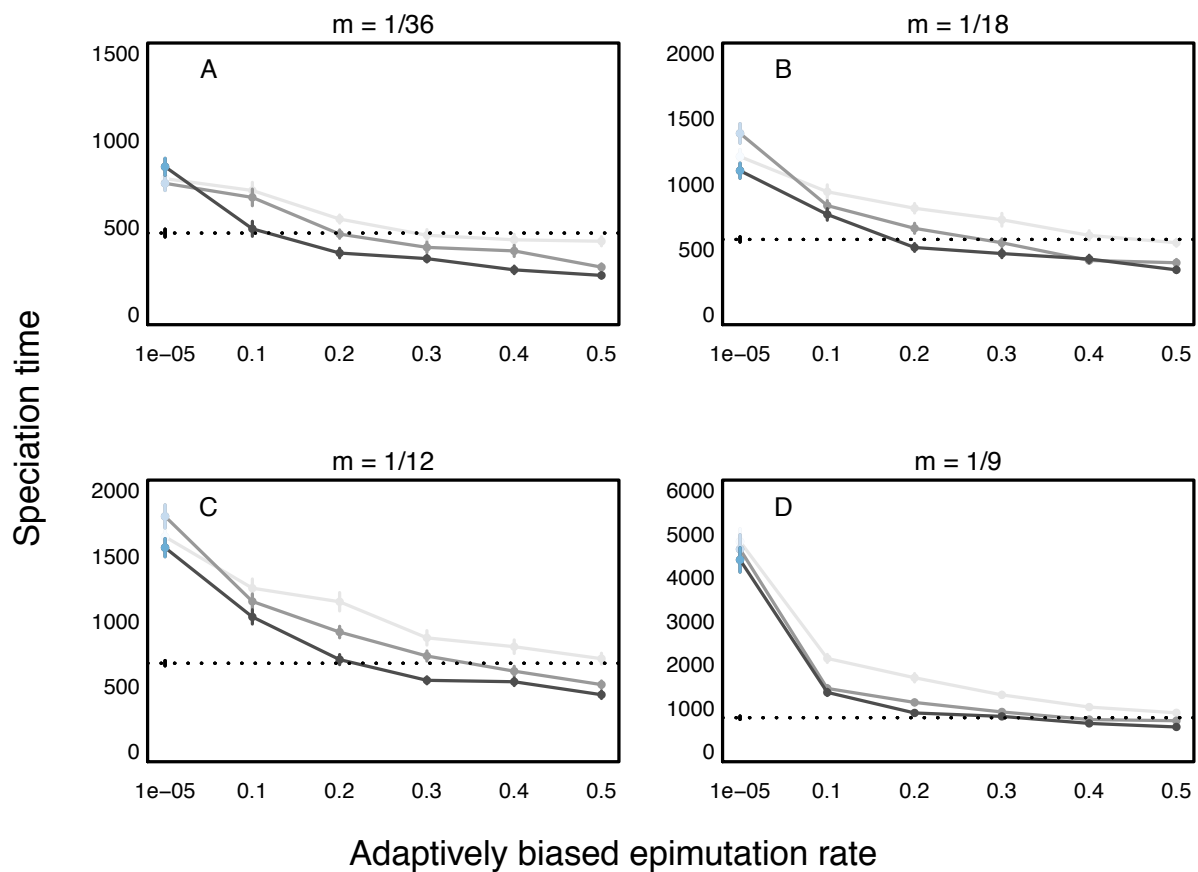


Figure S12: Analog of Fig. S4, but with lower migration rates. Parameters values are listed in Table 1, except  $\sigma = 0.4$ , with  $\tau = 1$  (light grey),  $\tau = 2$  (dark grey) and  $\tau = 3$  (black). The dotted line shows the time to speciation for a model with 20 genetic loci and no epigenetic loci. Note the differing scales for the  $y$ -axes among panels.

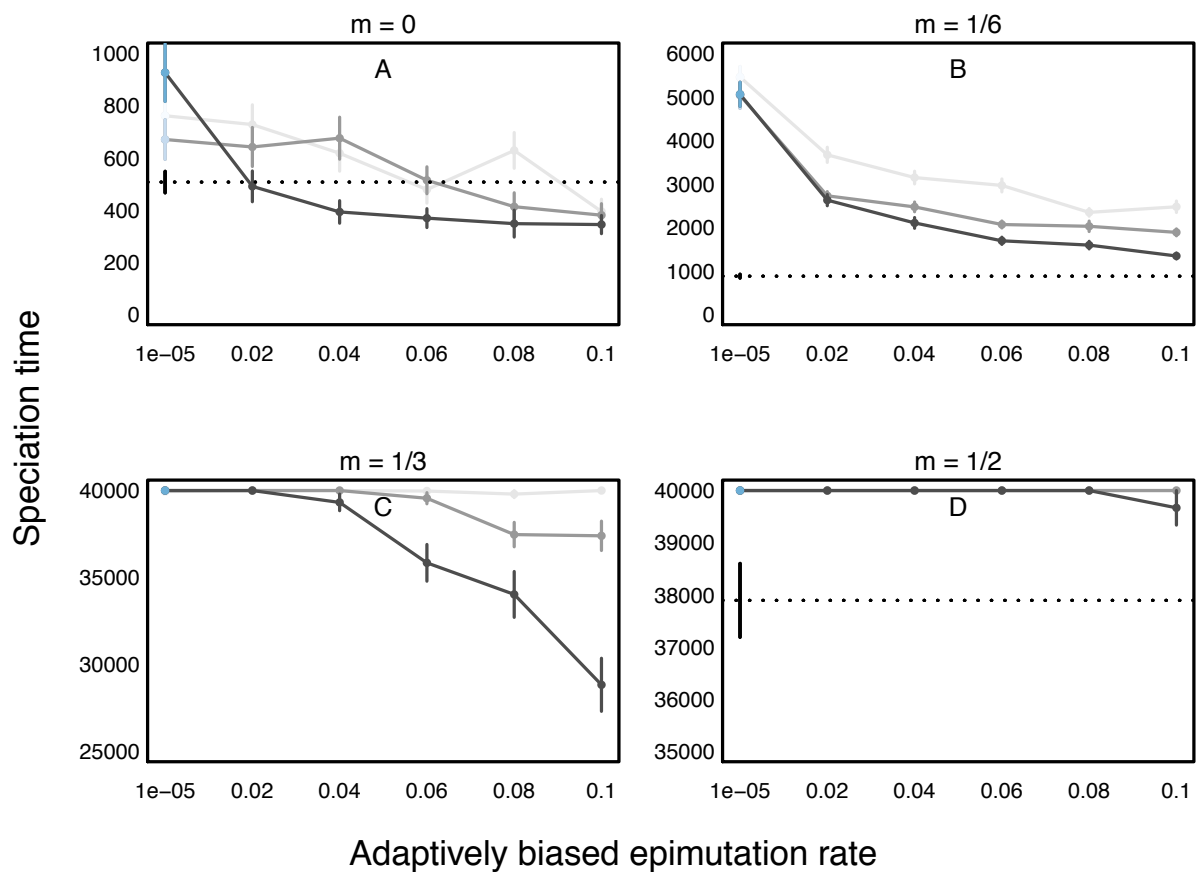


Figure S13: Analog of Fig. 2, but with smaller values of the adaptively biased epimutation rate. Parameters values are listed in Table 1 with  $\tau = 1$  (light grey),  $\tau = 2$  (dark grey) and  $\tau = 3$  (black). The dotted line shows the time to speciation for a model with 20 genetic loci and no epigenetic loci. Note the differing scales for the  $y$ -axes among panels.

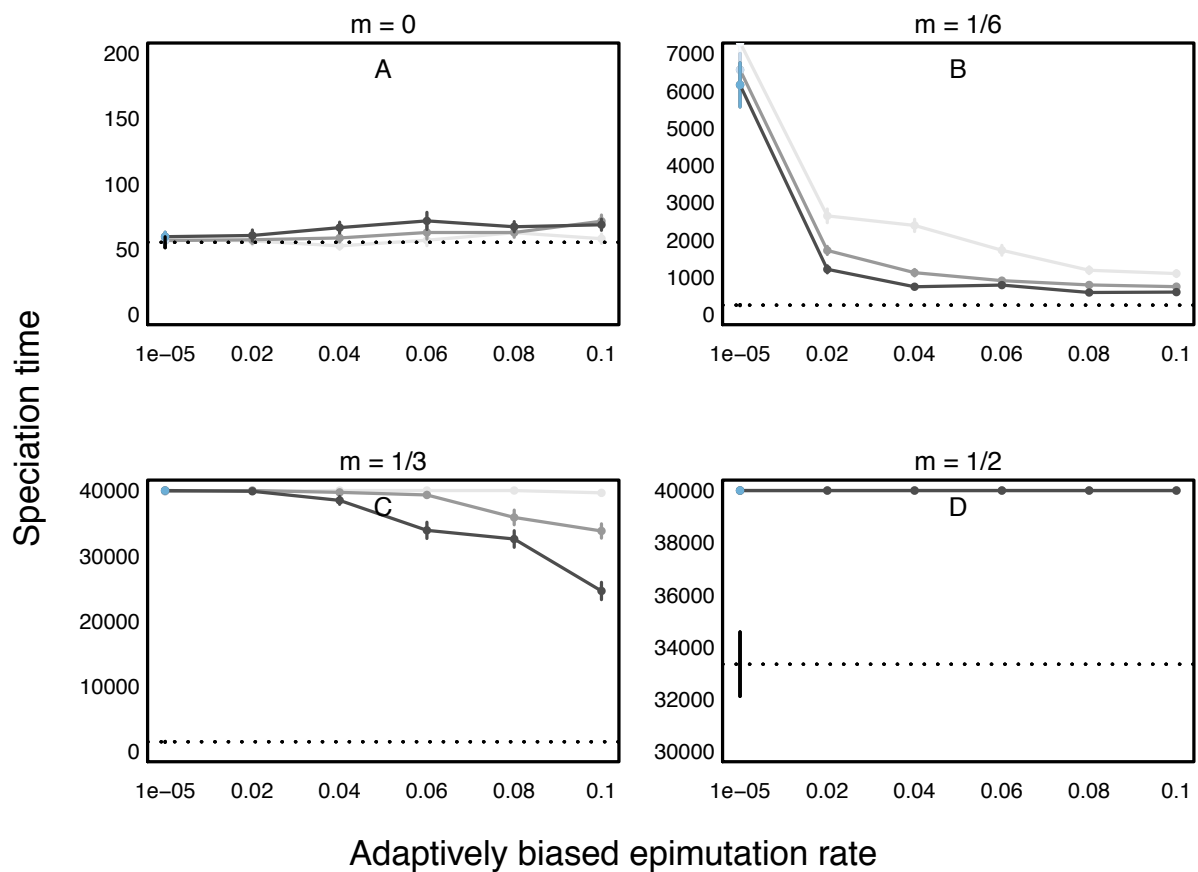


Figure S14: Analog of Fig. 4 (soft selection scenario), but with smaller values of the adaptively biased epimutation rate. Parameters values are listed in Table 1 with  $\tau = 1$  (light grey),  $\tau = 2$  (dark grey) and  $\tau = 3$  (black). Note the differing scales for the  $y$ -axes among panels.

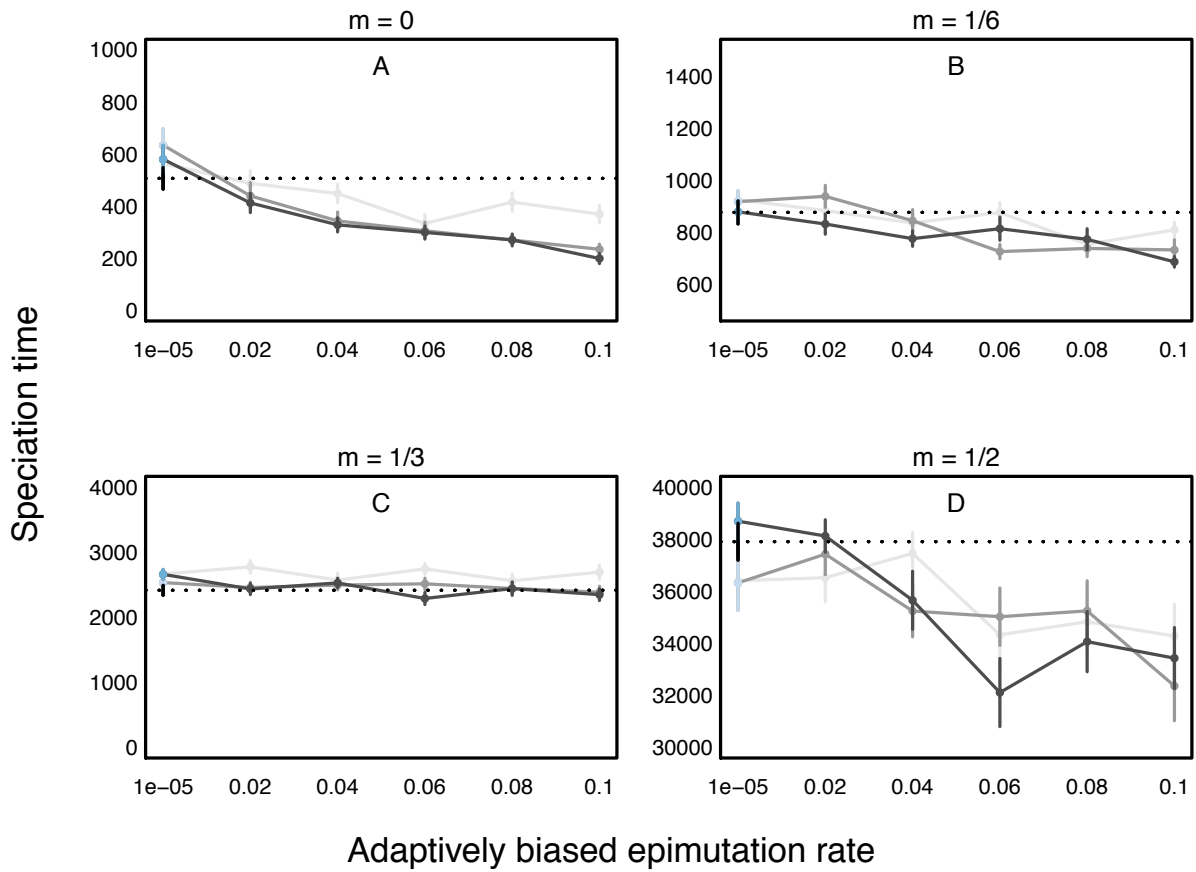


Figure S15: Analog of Fig. 5 (redundant map), but with smaller values of the adaptively biased epimutation rate. Parameters values are listed in Table 1 with  $\tau = 1$  (light grey),  $\tau = 2$  (dark grey) and  $\tau = 3$  (black). Note the differing scales for the  $y$ -axes among panels.

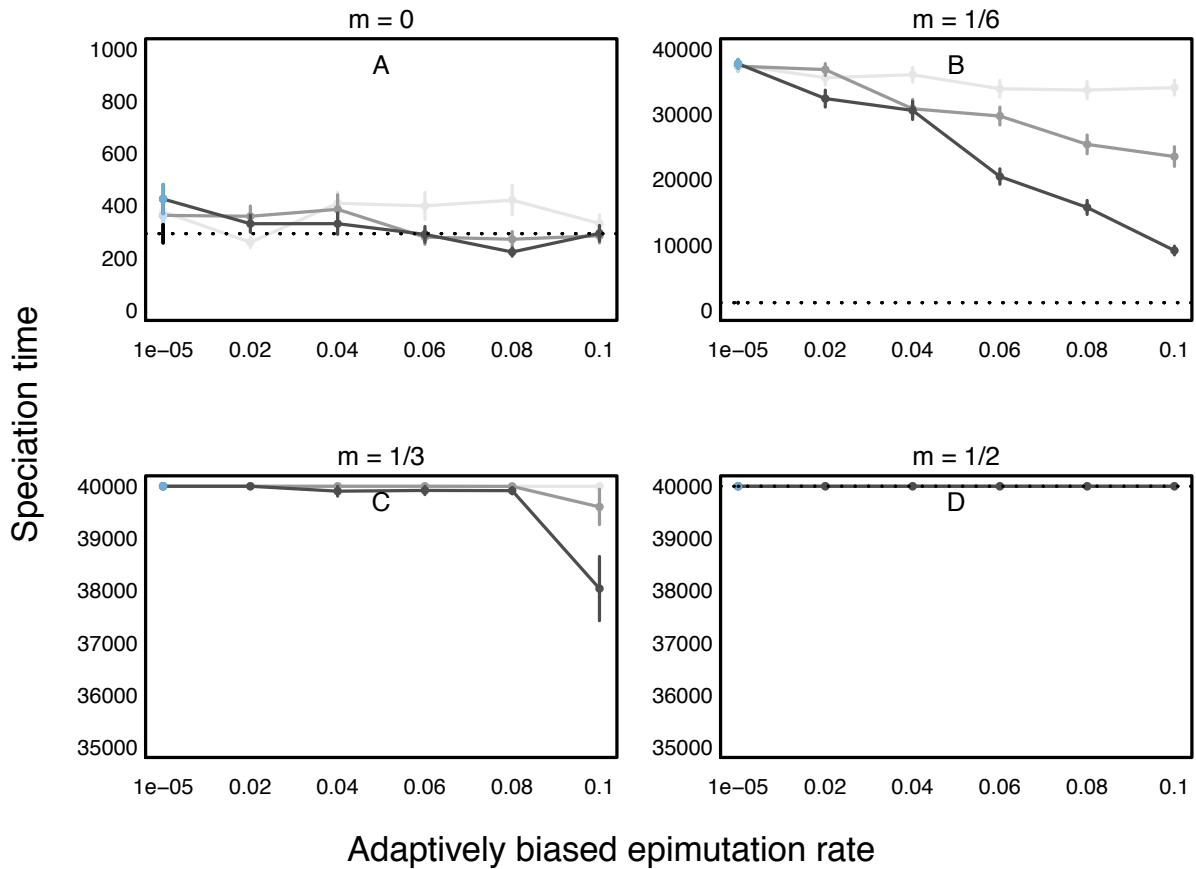


Figure S16: Analog of Fig. S4 (weak selection case), but with smaller values of the adaptively biased epimutation rate. The dotted line shows the time to speciation for a model with 20 genetic loci and no epigenetic loci. Parameters values are listed in Table 1, except  $\sigma = 0.4$ , with  $\tau = 1$  (light grey),  $\tau = 2$  (dark grey) and  $\tau = 3$  (black). Note the differing scales for the y-axes among panels.

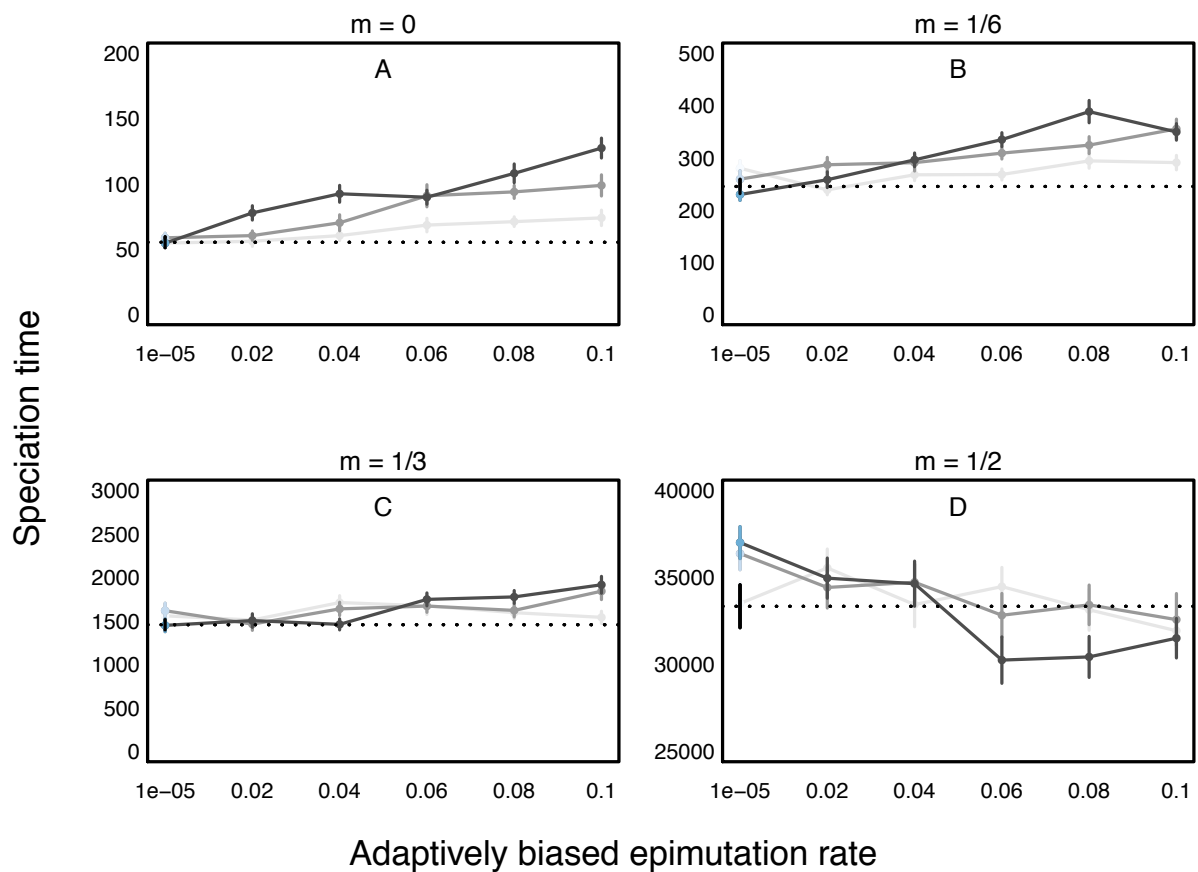


Figure S17: Analog of Fig. S8 (redundant map and soft selection), but with smaller values of the adaptively biased epimutation rate. Parameters values are listed in Table 1 with  $\tau = 1$  (light grey),  $\tau = 2$  (dark grey) and  $\tau = 3$  (black). Note the differing scales for the  $y$ -axes among panels.

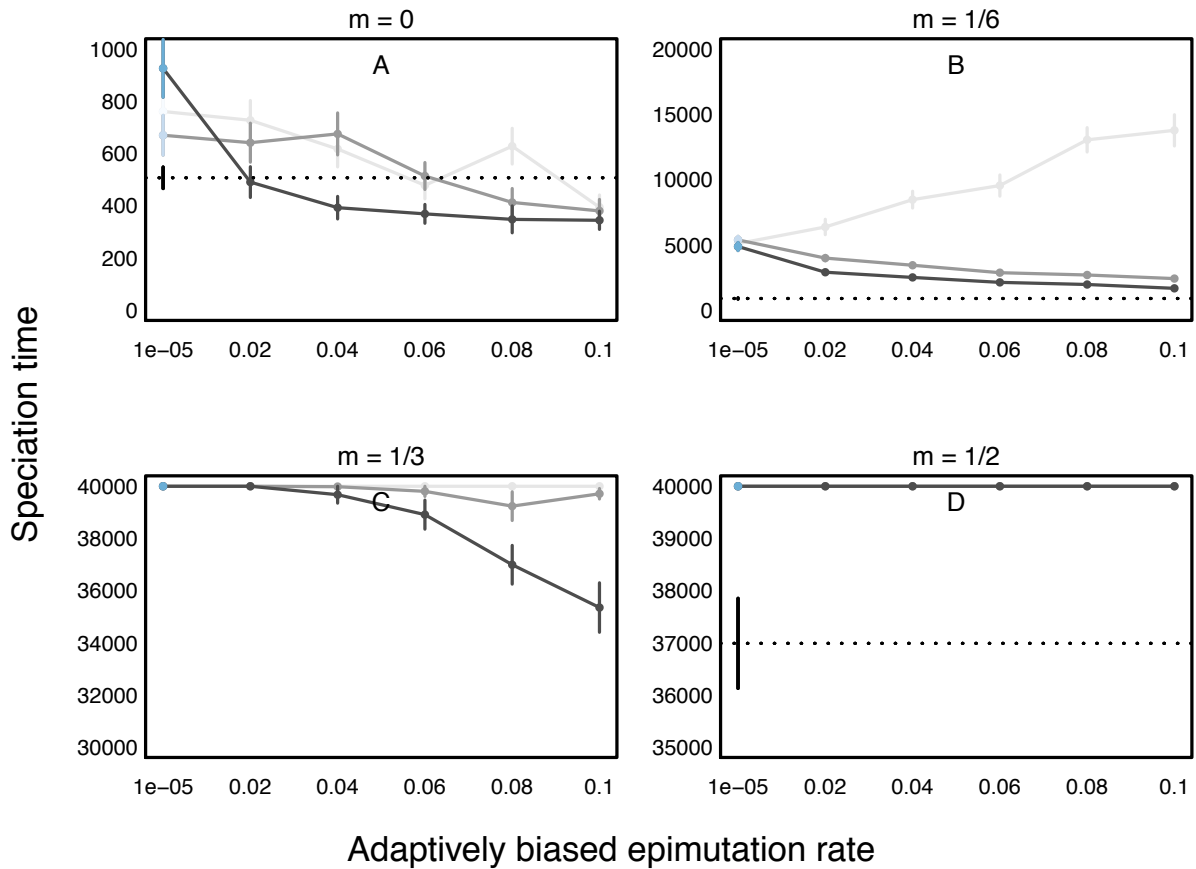


Figure S18: Analog of Fig. S9 (mutation after migration), but with smaller values of the adaptively biased epimutation rate. The dotted line shows the time to speciation for a model with 20 genetic loci and no epigenetic loci. Parameters values are listed in Table 1 with  $\tau = 1$  (light grey),  $\tau = 2$  (dark grey) and  $\tau = 3$  (black). Note the differing scales for the  $y$ -axes among panels.